ELSEVIER

Polymer 41 (2000) 6323–6334

polymer

High pressure capillary rheometry of polymeric fluids

M.A. Couch*, D.M. Binding

Department of Mathematics, University of Wales, Penglais, Aberystwyth, Ceredigion, Wales SY 23 3BZ, UK

Received 15 July 1999; received in revised form 29 October 1999; accepted 17 November 1999

Abstract

The application of superposition theory to capillary and entry pressure drop data for a number of polymer melts, measured at elevated pressures, is investigated in order to gain information on their pressure dependencies in both shear and elongational flows. To facilitate the study a capillary rheometer has been modified, by fitting a second chamber and valve arrangement below the main die, which allows the pressure downstream of the relevant capillary and orifice dies to be raised so that the mean pressure associated with each die can be varied. Five polymer melts are investigated: high-density polyethylene (HDPE), low-density polyethylene (LDPE), polypropylene (PP), polymethyl methacrylate (PMMA) and polystyrene (PS). Each of these are tested at three temperatures within the normal processing range, at apparent shear rates between 50 and 2500 s^{-1} and at mean pressures ranging from atmospheric up to 80 MPa. Time–temperature–pressure superposition is applied to the capillary and orifice pressure drop data for each of the polymers and the resulting pressure coefficients are found to be independent of temperature. The superposition is found to hold for all of the samples considered in both shear and elongational flow, although the degree of fit is best for the HDPE and LDPE. The resulting pressure coefficients for the shear and elongational flows then order the pressure dependencies of the polymers as follows: PS > PMMA > PP > LDPE > HDPE. It is demonstrated how this ordering is determined by the molecular structure of the polymers. However, the most significant result is that for each polymer the shear temperature and pressure coefficients are of similar value to those of elongation, with the exception of PS that has considerably greater coefficients in elongation particularly for temperature. Complementary results for single and multigrade oils are also included, in the appendix.

Keywords: Capillary rheometry; Polymeric fluids; Multigrade oils

1. Introduction

This paper follows up work carried out in a recent publication [1] by the same authors, who dealt with the pressure dependence of the shear and extensional viscosity of polymer melts. The current paper, however, focuses on the application of superposition theory to capillary and entry pressure drop data, obtained with a modified capillary rheometer, in order to gain information on the pressure dependencies of polymer melts in both shear and elongational flows.

Previously, work in this field has been confined to pressure dependence in shear flow (capillary or slit die) and no consideration has been given to the effects of pressure on elongational (entry) flows. A robust review of this earlier work is included in the literature review of the previous paper.

In addition to pressure dependence, the present study will also assess the influence of temperature together with the interrelationships between temperature and pressure, via the application of time–temperature–pressure superposition. The resulting findings are, therefore, expected to be of importance to the field of polymer processing where variations of temperature and pressure will have significant repercussions on the polymer's rheometric properties, since these properties are strong functions of both temperature and pressure.

2. Theory

It is well established that the viscosity of most polymer melts is well represented by an exponential function of pressure. This pressure dependence was first defined by the now well-known Barus equation [2]:

$$\eta = \eta^{(0)} e^{\beta P}, \tag{1}$$

where $\eta^{(0)}$ is the viscosity at ambient pressure, β is the pressure coefficient and P is gauge pressure. However, there have not been many reliable measurements of the coefficient of pressure dependence of viscosity, β, which is a difficult quantity to measure. An average value for polymer

* Corresponding author.

0032-3861/00/$ - see front matter
PII: S0032-3861(99)00865-4

melts taken from the literature is estimated to be of the order of 20 GPa^{-1}.

Viscosity is also known to have an exponential dependence on temperature, which can be expressed, for example, through the Arrhenius expression (for Newtonian fluids):

$$\eta = B\, e^{E/RT}, \tag{2}$$

where E is the activation energy, R is the gas constant and T is the absolute temperature. This type of equation is usually suitable for describing the variation of viscosity with temperature provided the range of temperature is not very large. For analytical work it can be rewritten in the more useful form:

$$\eta = \eta_R \exp\frac{E}{R}\left(\frac{1}{T} - \frac{1}{T_R}\right), \tag{3}$$

where T_R is a convenient reference temperature and η_R is the viscosity at the reference temperature. An alternative empirical equation that is more accurate over wider ranges of temperature is the Vogel equation [3]:

$$\eta = A_1 \exp\frac{B_1}{T - T_R}, \tag{4}$$

where A_1, B_1 and T_R are constants. These expressions are useful provided the temperature is appreciably higher than the glass transition temperature T_g. Near to T_g the dependence is better described by the familiar WLF (Williams–Landel–Ferry) equation [4], which is based on the dependence of viscosity upon free volume described by the Doolittle equation [5].

Defining E/R or β through the above equations is adequate when dealing with Newtonian fluids, but is not suitable for viscoelastic materials, as the expressions do not account for strain rate dependence. Consequently, this will lead to coefficients that vary with strain rate. In order to get around this difficulty, it is convenient to define temperature and pressure dependence in the following way. By way of example, consider the shear stress function $\sigma(\dot\gamma, T, P)$, which is a function of shear rate, $\dot\gamma$, as well as temperature, T, and pressure, P. We define the parameter a_{TP}^S by:

$$\sigma(\dot\gamma, T, P) = \sigma(a_{TP}^S \dot\gamma, T_R, P_R), \tag{5}$$

where P_R and T_R are a reference pressure and reference temperature, respectively. If a_{TP}^S is found to be independent of shear rate (that is, dependent only on pressure and temperature), we say that the shear stress satisfies the time–temperature–pressure superposition. We may define an analogous parameter a_{TP}^E for the tensile stress. If superposition holds for the shear stress one would expect it to hold for the tensile stress as well. Indeed, if superposition holds for a particular material it might be expected that $a_{TP}^S = a_{TP}^E$.

As stated in the introduction rheological properties are typically highly dependent on temperature and pressure. Thus, to obtain a full picture of the behaviour, experiments must be carried out over a range of temperatures and pressures. Data, for example shear viscosity versus shear rate, obtained under these conditions often can be brought onto a single master curve by means of the "time–temperature–pressure superposition", which greatly simplifies the description of the effects of temperature and pressure. Further, it facilitates the display of data on a single curve of material behaviour that covers a much broader range of time (or frequency, or strain rate, etc) than can be measured at a single temperature or pressure.

The theory of superposition is based on the concept that all the relaxation processes of a particular material have the same dependence on either temperature or pressure. Both temperature and pressure are assumed to affect the relaxation modulus by changing all the relaxation times by the same factor a_{TP}, which is dependent on temperature and pressure. For a more detailed discussion of the temperature and pressure dependence of viscoelastic behaviour, see Ferry [4].

The function a_{TP} cannot be predicted from first principles, but it can be determined empirically as a shift factor. For example, in the case of the shear viscosity function $\eta(\dot\gamma)$ temperature/pressure independent representations can be prepared by plotting $\eta(\dot\gamma)/a_{TP}$ versus $a_{TP}\dot\gamma$ on a double logarithmic plot. Alternatively, this can be done more simply in terms of the shear stress function by plotting $\sigma(\dot\gamma)$ versus $a_{TP}\dot\gamma$[1] and in the current case of capillary flow pressure drop data can be substituted for the shear stress since they are directly proportional. The shift factor can then be determined by examining the amount of shifting necessary to bring data taken at different temperatures and pressures onto one curve. In our case, the shift factors are determined automatically by an iterative procedure, developed in-house. In the present study the shift factors a_{TP} are found to be well represented by a combination of Barus and Arrhenius terms given by Eqs. (1) and (3) such that:

$$a_{TP} = \exp\left[\beta_{P+}\frac{E}{R}\left(\frac{1}{T} - \frac{1}{T_R}\right)\right]. \tag{6}$$

Thus, the temperature and pressure dependencies of a given polymer can be determined by finding those values of E/R and β that yield the best overall fit to the associated master curve. In the data manipulation we do NOT assume, a priori, that the parameters E/R and β have the same values for both the shear and elongational properties.

Note that, in the previous paper [1], values of β were calculated by a different method, which simply involved assessing the extent of the exponential shift of viscosity with pressure, as defined by the Barus equation (1). Normally this would be problematic since the pressure coefficients, when calculated in this way, would vary with shear rate (certainly for non-Newtonian fluids). However, since

[1] There is an equivalent shift factor associated the shear stress term σ, but this is dependent on the density of the fluid, which does not vary significantly along the length of the capillary. Therefore this factor is assumed to be negligible in the present case.

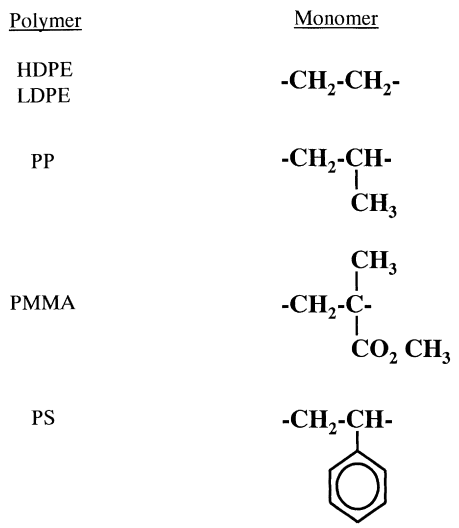

Fig. 1. Structural formulae of the polymers.

the recorded data was in the power-law region, i.e. the relevant curves were parallel, constant values of β were obtained for each polymer. This method was adopted because it emphasises the difference between the shear and elongational pressure coefficients at a given strain rate, which is useful when calculating the pressure dependence of the Trouton ratio. A basic relationship exists between the βs calculated by this ('Barus') method and the current (superposition) procedure involving the power-law indices of the shear and extensional viscosity curves n and t, such that:

$$\beta_S(\text{Barus}) = n\beta_S(\text{super}) \quad \text{and} \quad \beta_E(\text{Barus}) = t\beta_E(\text{super}). \tag{7}$$

Here the subscript S denotes shear and E elongation.

3. Polymer structure

In general, the rheology of all flexible chain polymers is remarkably similar, because the chains are very long and flexible and the paths of the moving chains cannot cross those of their neighbours. In the absence of a deforming stress, the flexible polymer chains take the shape of random coils. These coils are viscoelastic in nature, i.e. when they are exposed to an external stress they undergo strain, but relax fully when the stress is removed, although the relaxation is retarded by molecular friction that arises from the intermolecular forces. As there is considerable overlapping between the coils, the motion of any individual molecule is strongly effected by the presence of its neighbour.

In practice the motion of the individual atoms within the coils, and hence the coil structure, is influenced by the presence of other atoms, either on the backbone chain of carbon atoms or on groups of atoms attached to the backbone. For example the presence of strong interactions or of bulky pendant groups attached to the backbone will stiffen the polymer chain and make it less flexible. The strength of the interactions with other atoms depends on the detailed molecular structure of the polymer and is directly responsible for its physical properties. Thus, the rheological behaviour (e.g. viscosity, elasticity, temperature and pressure dependence) of a given polymer will depend on a combination of its molecular structure and molecular weight distribution.

For the vast majority of polymer melts the zero shear viscosity η_0 is solely dependent on the average molecular weight M_w of the polymer and is completely independent of the molecular weight distribution MWD. If the molecular weight of the polymer is above a critical level, which varies with the molecular structure of each polymer, then the role of entanglements becomes important and the dependence of η_0 on M_w becomes much more pronounced. In contrast, the variation of viscosity with shear rate, particularly the onset of viscoelasticity and the power-law slope, is very dependent upon the molecular weight distribution. In general, polymers with broad molecular weight distributions exhibit the onset of shear thinning at low shear rates.

In contrast, the temperature and pressure dependence of the viscosity of polymer melts is determined by their molecular structure. An increase in pressure or a decrease in the temperature of a melt will result in a reduction in the availability of space, i.e. the free volume, between molecules. The increased proximity of the molecules will in turn lead to an increase in the number of interactions occurring during flow. This causes a corresponding rise in intermolecular friction and a subsequent increase in the viscosity of the polymer. As mentioned above, the molecular structure of the polymer molecules determines the shape and flexibility of the coils. Therefore, polymers whose structures are more susceptible to increased levels of molecular interaction will generate larger intermolecular forces under these conditions and thereby show greater viscous enhancement; i.e. these polymers will exhibit greater temperature and pressure dependence.

In the present study, we shall report on a number of commercial polymer melts. Five mainstream polymer processing grades were chosen: high-density polyethylene (HDPE) (BASF, Lupolen 1840H 5431P); low-density polyethylene (LDPE) (BASF, Lupolen 1840H); polypropylene (PP) (ICI, GWM 213)); polystyrene (PS) (BASF, Polystyrol 143E) and polymethyl methacrylate (PMMA) (ICI, CLH 374).

The structures of the monomer units that make up the polymers being studied are shown in Fig. 1. With regard to the polyethylene samples, both HDPE and LDPE are composed of long chains of the ethene (ethylene) monomer. HDPE is linear and, therefore, it has the simplest structure possible for a polymer. It is also of lower molecular weight than LDPE. On the contrary, LDPE exhibits long chain branching. Such polymers are known to have greater temperature/pressure dependence than linear polymers of

the same chemical structure, although the reasons for this are not yet well understood. PP has a methyl group attached to the backbone chain of its monomer unit. These side groups are usually arranged in isotactic form, i.e. each asymmetric chain atom has its substituents in the same steric order. The above polymers are of crystalline structure, though the degree of crystallinity of the polyethylenes is controlled by the chain structure (branching). PMMA has a methyl group and a larger methacrylate group attached to its carbon chain, while PS has an even larger benzene ring as its pendant group. Both these molecules are normally atactic in form, i.e. the steriochemistry of the tertiary carbon atoms in the chain is random. They are also of non-crystalline structure (amorphous). As mentioned above, the large pendant groups of the PS and PMMA tend to make these molecules more rigid and, hence, elongated.

4. Experimental

Full details of the high-pressure instrument and experimental procedure are given in Ref. [1], although the key points are summarised below.

The instrument used to carry out the experiments is a prototype capillary rheometer capable of operating at pressures of up to 140 MPa and a temperature range from 20 to 500°C. It has been modified by the addition of a second chamber fitted below the die of one of the two rheometer barrels as shown in Fig. 2. At the base of the chamber is a constriction made up of a conical die and a conical plug. The plug can be moved vertically by means of a screw thread in order to vary the level of constriction in the die, thereby controlling the back pressure in the chamber. Pressures up and down stream of the die are monitored by flush mounted pressure transducers rated at up to 140 MPa, while the temperature control of the chamber is maintained by a separate system to that of the barrel. In order to cope with the high pressures, the piston is also modified by fitting a PTFE washer to its brass head, which is squeezed out to form a tight seal against the barrel wall when pressure is applied to the end of the piston. The rheometer can deliver a constant ram/piston speed, which generates a constant flow rate throughout the instrument geometry (once steady state conditions are achieved.) The constriction can then be adjusted to control the pressure in the second chamber and the upstream and downstream pressure transducers used to measure the total pressure drop associated with the die.

Each of the polymers was tested at three convenient temperatures within the normal processing range. Two dies were employed: a capillary of diameter 1 mm and length 25 mm and an orifice of the same diameter, but of nominally zero length. Mean pressures for all the polymers were limited to a maximum of around 70 MPa, to avoid problems with crystallisation etc. A tip-sensitive temperature probe was used to check that isothermal conditions were maintained along the length of the melt barrel and in the second chamber. The high-pressure experiments were initiated by selecting a fixed ram speed at which the melt was pushed through the die with the constriction fully open. Both transducer readings were recorded simultaneously once the pressures had stabilised. The constriction was then tightened, which resulted in the elevation of both the barrel and chamber pressures. Once the chamber had reached a stable pre-determined pressure, the pressures were again recorded. The chamber pressure was incremented in this way from ambient up to the maximum used for several flow rates between 4.91×10^{-9} and 2.45×10^{-7} $m^3 s^{-1}$.

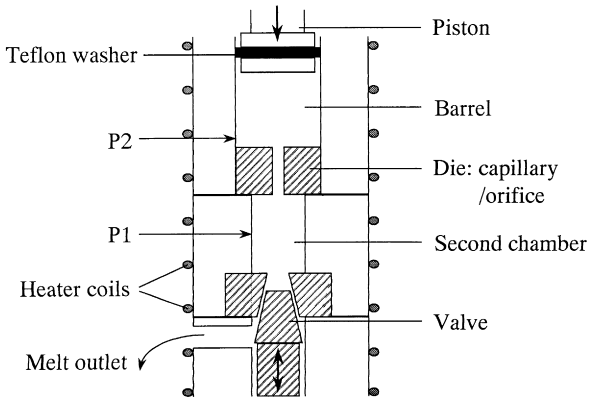

Fig. 2. Schematic diagram of the modified "high pressure" capillary instrument.

This procedure has the disadvantage that the relevant pressure drops associated with the capillary (or orifice) are not directly controlled. Consequently, the analysis of the data is more complex than it would be otherwise. The next section details the procedures used for analysing the experimental data.

5. Data interpretation

Fig. 3 shows a schematic diagram of the entry and exit flow regions around the orifice and the capillary dies for a

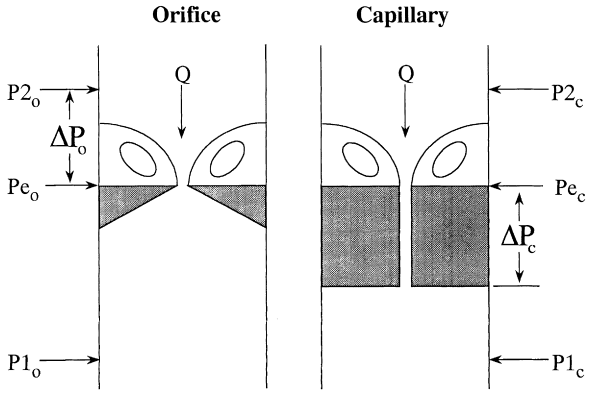

Fig. 3. Schematic diagram of the entry and exit flow regions around the orifice and capillary dies.

melt flowing at a constant flow rate Q. Also featured on the diagram are the pressure levels at the transducers and the entrances to the dies. The pressure drop associated with the entry flow to the orifice ΔP_o is simply defined as the difference in pressure between the upstream transducer level $P2_o$ and the value at the orifice entrance Pe_o :

$$\Delta P_o = P2_o - Pe_o. \tag{8}$$

Assuming that the *exit* pressure losses are negligible, the pressure at the downstream transducer $P1_o$ will be equal to the entrance pressure and so:

$$\Delta P_o = P2_o - P1_o. \tag{9}$$

Note that the assumption that the exit pressure drop is negligible in comparison with the entry pressure drop is quite common in capillary rheometry, (see, for example Carreau [6] or Moldenaers et al. [7]). In order to get a measure of the actual pressure associated with the orifice pressure drop a mean value $\bar{P}_o$of the two measured pressures is taken:

$$\bar{P}_o = \frac{1}{2}[P2_o + P1_o]. \tag{10}$$

The pressure drop along the capillary ΔP_c is taken as the difference between the pressure at entry, Pe_c and the downstream pressure $P1_c$:

$$\Delta P_c = Pe_c - P1_c. \tag{11}$$

However, the pressure drop needs to be expressed in terms of the upstream pressure $P2_c$ as the entry pressure cannot be measured directly. In practice, this is achieved by applying the so-called Bagley correction [8,9]. The main premise of this correction is that the entry flows, to the orifice and to the capillary, are essentially the same at the same flow rate and that they generate the same pressure drop. In our case this condition will only hold, provided the upstream pressures, as well as the flow rates are equal. This can always be achieved, in principle, by adjusting the downstream pressure using the valve. In practice, however, it is easier to set convenient downstream pressures and then to interpolate the upstream data to obtain the relevant pressure drops. Thus, the capillary entry pressure is obtained by subtracting the orifice pressure drop, determined at the corresponding upstream pressure ΔP_o ($P2$) from the capillary upstream pressure. Eq. (10) then becomes:

$$\Delta P_c = \{P2_c - \Delta P_o(P2)\} - P1_c. \tag{12}$$

By similar reasoning the mean pressure in the capillary $\bar{P}_c$ is given by:

$$\bar{P}_c = \frac{1}{2}[P2_c - \Delta P_o(P2) + P1_c]. \tag{13}$$

Once the pressure drops have been determined as a function of pressure it is possible to obtain temperature and pressure coefficients for shear and elongational flow by applying the time–temperature–pressure superposition to the raw data as follows: The orifice and capillary pressure drops are first plotted against apparent shear rate at all three temperatures for each of the polymers. Although it is more conventional to plot orifice pressure drop data versus flow rate, Maia and Binding [10] have suggested that it can be advantageous to plot against rim shear rate. In a study of the entry flows of polymer solutions they found that their orifice pressure drop data, measured with several dies of different diameter, all collapsed onto one curve when plotted against rim shear rate. The apparent shear rate $\dot{\gamma}_A$ for both the capillary and orifice is determined from the equation:

$$\dot{\gamma}_A = \frac{4Q}{\pi R^3}, \tag{14}$$

where Q is the volume flow rate and R is the die radius. A single shift is then performed along the time axis using the shift factor a_{TP} introduced in Section 2. An iterative technique is employed to ensure that the best fit for the temperature and pressure coefficients are obtained from the data. Note—although these coefficients are obtained from the raw orifice and capillary pressure drop data they actually represent the coefficients for shear and elongation, due to the dominance of shear in capillary flow and extension in entry flow. Hence, the subscripts S and E are applied to the temperature and pressure coefficients to denote either shear or elongation.

Shear viscosities for the polymer melts are calculated from the superimposed capillary pressure drop data by first fitting a polynomial (usually third order) to the (log) capillary data and then applying the conventional equations of capillary rheometry, incorporating the Weissenberg–Rabinowitsch correction [11].

The analysis assumes that the pressure gradient along the length of the capillary, although non-linear due to the pressure dependant viscosity, can be approximated by $\Delta P_c/L$, the total pressure drop over the capillary length. In fact, Penwell et al. [12], have developed an expression for the axial pressure distribution along a capillary, based on an exponential dependence of shear viscosity on pressure, which is:

$$P(z) = \ln[e^{-\beta\Delta P} + (1 - e^{-\beta\Delta P})z/L] - \beta, \tag{15}$$

where $P(z)$ is the pressure, β is the pressure coefficient, ΔP is the total pressure drop, z is the displacement along the capillary and L is the full capillary length. This model predicts a concave pressure profile along the capillary, but, provided the overall pressure drop for the capillary is relatively modest or the pressure coefficient is small, the deviation from the linear case is small and a linear approximation for the pressure gradient is justifiable.

Similarly the superimposed orifice pressure drop data can be used to obtain estimates of the extensional viscosity for the polymer melts. That work is not included in the current study but is the main subject of an earlier paper [1].

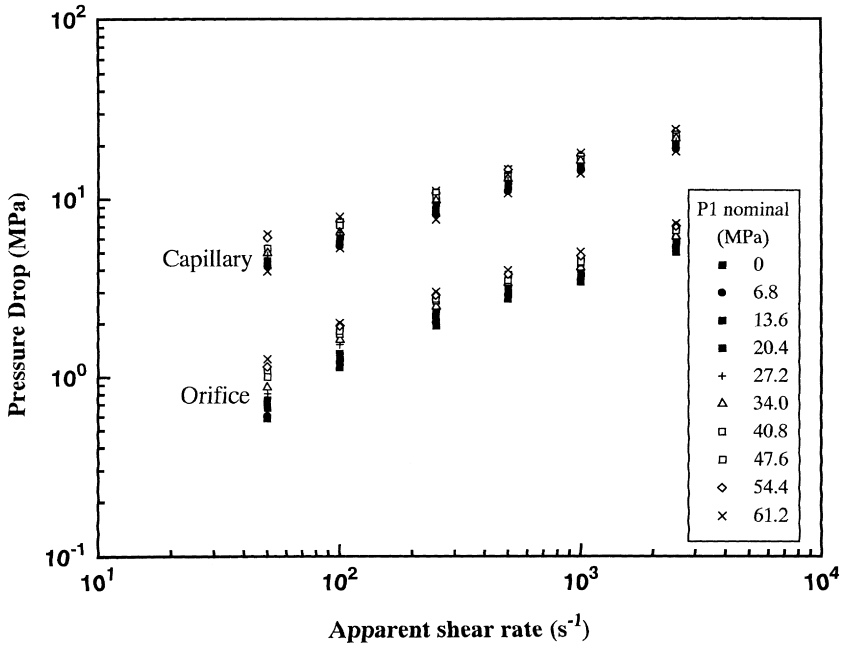

Fig. 4. Raw orifice and Bagley-corrected capillary pressure drop versus apparent shear rate data for LDPE at 200°C.

6. Experimental results

6.1. Low-density polyethylene

Tests on LDPE were carried out at three different temperatures: 170, 200 and 230°C. Examples of how the orifice and capillary pressure drops vary with mean pressure at 200°C are given in Fig. 4. Here the raw data are plotted together as a function of apparent shear rate, in order to make direct comparison easier. The apparent shear rate range investigated is relatively high for LDPE having a maximum level of $2.5 \times 10^3\ s^{-1}$. However, this is no greater than the ranges used by Laun [13] or Kadijk and van den Brule [14] who covered ranges up to 2×10^3 and $3 \times 10^3\ s^{-1}$, respectively, in their studies on high pressure shear rheometry using slit dies.

For further convenience, the pressure drop data points are plotted with reference to the nominal downstream pressure $P1$ to avoid the complication of specifying an individual mean pressure for every point. Though the graph is on a logarithmic scale, the pressure drops are evenly spaced with each increment of nominal pressure (which is on a

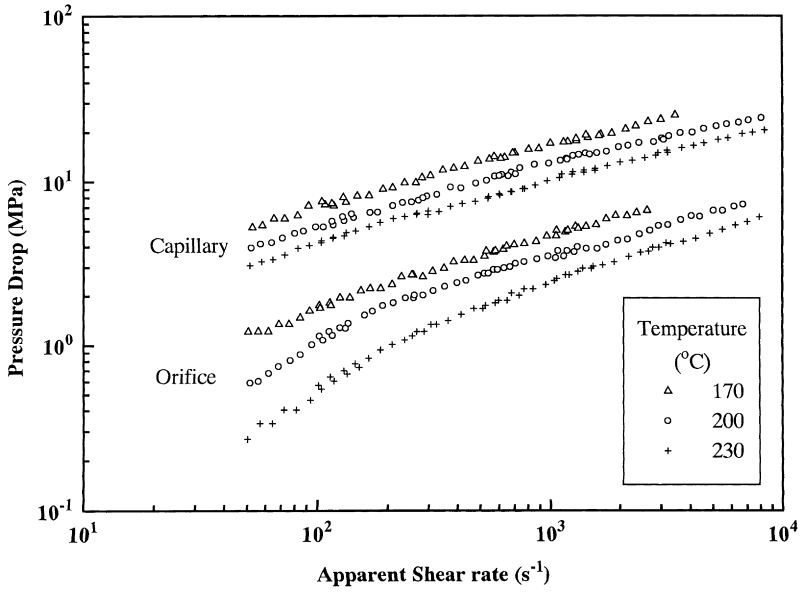

Fig. 5. Pressure reduced orifice and capillary data for LDPE at 170, 200 and 230°C.

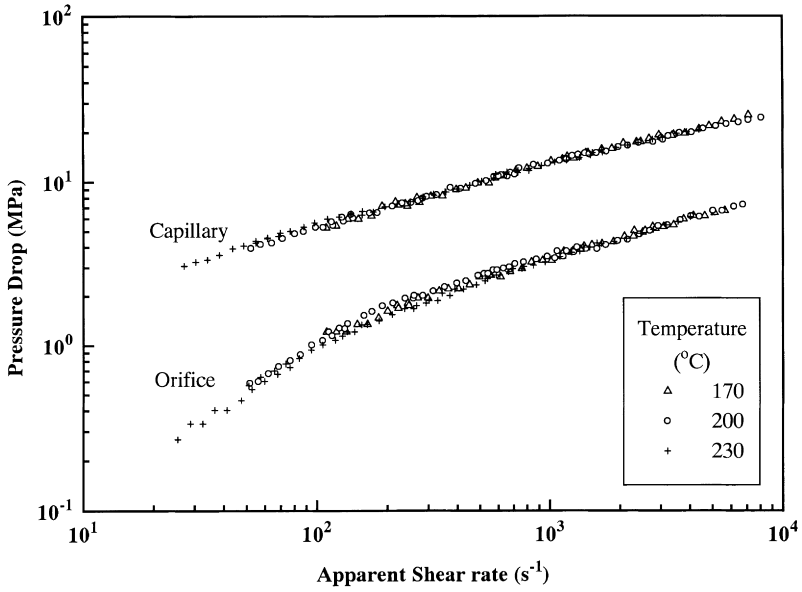

Fig. 6. Temperature and pressure reduced orifice and capillary data for LDPE.

linear scale.) This indicates that both the orifice and capillary pressure drops have an exponential dependence on pressure over the range of measured flow rates. Only a fairly modest increase of approximately 50% in the pressure drops is observed over the pressure range investigated. However, Laun [13] failed to record any increase in the entrance pressure loss of a slit die for LDPE over a similar range of pressures.

Subsequently, the orifice and capillary data (at 200°C) are superimposed, via the mechanism outlined in the data interpretation section, and then plotted alongside equivalent superimposed data for 170 and 230°C in Fig. 5. The level of temperature dependence is fairly modest in this case.

Full time–temperature–pressure superposition for the LDPE is illustrated in Fig. 6. This provides direct evidence that the a_{TP} parameter, as defined, is independent of shear rate, for the range of temperatures and pressures used. Note that for this and all the other polymers the reference temperature T_R was selected as 200°C (the middle temperature for LDPE) in order to facilitate later comparisons between the polymers. The reference pressure is atmospheric.

The shifting procedure leads to the extension of the range of shear rates covered from 1(1/2) (see Fig. 4) to over 2(1/2) decades (see Fig. 6). Good superposition is observed for most of the data with an error margin estimate of typically less than 3% for those of the capillary, although greater scatter is observed with the orifice at the lowest shear rates and pressures due to the relatively small values of the pressure drops.

Both sets of pressure drops exhibit power-law behaviour at the higher shear rates, although some curvature in the logarithmic plots is apparent particularly in the case of the orifice data at the lower shear rates and pressures.

The best-fit values of the coefficients β and E/R for LDPE are obtained by fitting Eq. (6) to the determined shift parameters. The values are recorded in Tables 1 and 2, respectively, together with the equivalent coefficients for the other polymers. Both the temperature and pressure coefficients are moderate and the shear and elongational cases have similar values to each other. It is interesting that the shear pressure coefficients recorded at 15–17 GPa^{-1} are only marginally lower than that of Laun [13] who arrived at a shear pressure coefficient of 20 GPa^{-1} for LDPE, based on the curvature of the parabolic pressure profile in a slit die.

Table 1
Shear and extensional pressure coefficients for the five polymer melt samples

Melt	Temperature (°C)	β_S (GPa^{-1})	β_E (GPa^{-1})
HDPE	150	9.5	11
	170	10	10
	200	10.5	11.5
LDPE	170	16.5	15
	200	16	15.5
	230	17	16.5
PP	190	22.5	23.5
	200	22	23
	230	21.5	24
PMMA	220	25	29
	230	24	26
	240	25	28
PS	180	30.5	39
	200	29	37
	230	28	35.5

6.2. Polystyrene

Tests on PS were conducted at temperatures of 180, 200

Table 2
Shear and extensional temperature coefficients for the five polymer melt samples

Melt	α_S (°K)	α_E (°K)
HDPE	3600	3200
LDPE	5100	5400
PP	5400	6000
PS	9500	14,000
PMMA	12,500	14,500

and 230°C. Raw data for the orifice and capillary pressure drops of PS recorded at 200°C are plotted as a function of apparent shear rate in Fig. 7. The levels of pressure dependence, exhibited by both sets of data, are considerably higher than those obtained for LDPE. This is particularly true in the case of the orifice pressure drop, which experiences a four-fold increase over the measured range of mean pressures and become nearly as large as the capillary pressure drops at high shear rate and mean pressure.

This result has a significant bearing on conventional capillary rheometry measurements. The Bagley correction is normally carried out by subtracting orifice, or short capillary, pressure losses from those of the capillary, at corresponding flow rates. However, both sets of measurements are normally made with the die exits at ambient pressure. If the pressure drop along the capillary is significant then the actual entry pressure drop will be enhanced due to the elevated pressure conditions upstream of the capillary and will be underestimated by the Bagley correction. Consequently the resulting shear viscosity will be overestimated, particularly at high shear rates and with highly viscous or pressure dependent materials.

Pressure superimposed data obtained from Fig. 7 using the same technique employed for LDPE, together with equivalent data for the temperatures of 180 and 230°C, are shown in Fig. 8. The superposition attained with the capillary is, again, very good and the only significant scatter is again observed with the orifice at the lowest pressure drops, which coincide with the highest temperature and lowest shear rates. From this graph, it is apparent that the levels of temperature dependence for PS are also high, especially for the orifice.

Full superposition is shown in Fig. 9. The temperature superposition for PS is nearly as good as for the LDPE, except for the lowest temperature of 180°C at the highest shear rates. However, the range of shear rates covered is even greater than for LDPE at about three decades, which is a direct consequence of the higher levels of temperature and pressure dependencies. The pressure coefficients calculated for the capillary are substantial at 29 GPa^{-1}, while those of the orifice are even higher at 36 GPa^{-1}.

The values obtained for the shear coefficients are in fact very close to those found for PS by Penwell et al. [12] and Kadjik and Van den Brule [14] at 29 and 31 GPa^{-1}, respectively. Note that Kadjik and Van den Brule applied exponential shifts to shear data to obtain superposition and adopted a generalised Arrhenius–WLF equation to describe the exponential shifts, whereas Penwell et al. considered the non-linearity of Bagley plots. The temperature coefficients are also large and in the case of the orifice, they are over a third greater than those of the capillary.

It is felt that it is significant that the values of both E/R and β are larger for the orifice data than for the capillary whereas for all the other polymers, the values are similar for both orifice and capillary. This result is unexpected.

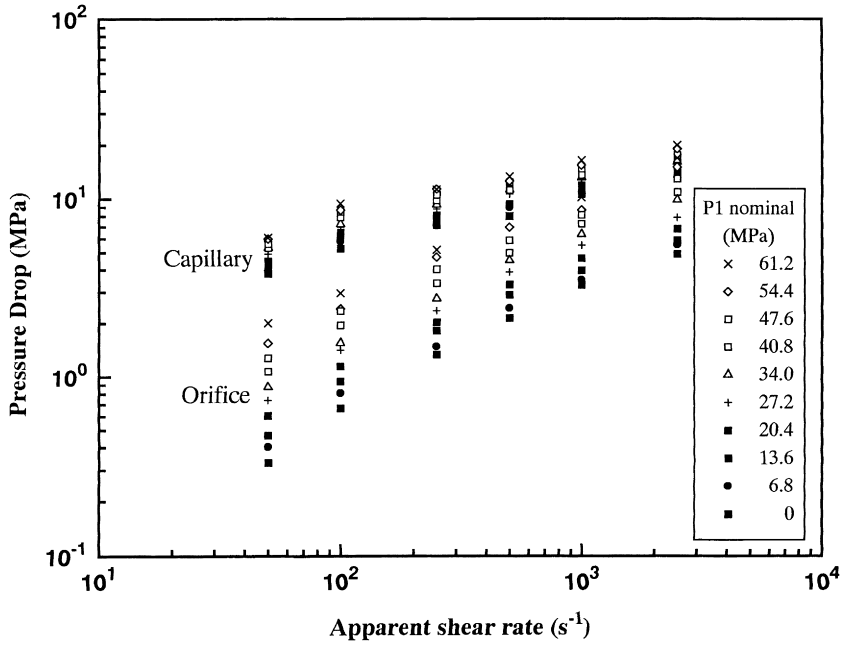

Fig. 7. Raw orifice and Bagley-corrected capillary pressure drop versus apparent shear rate data for PS at 200°C.

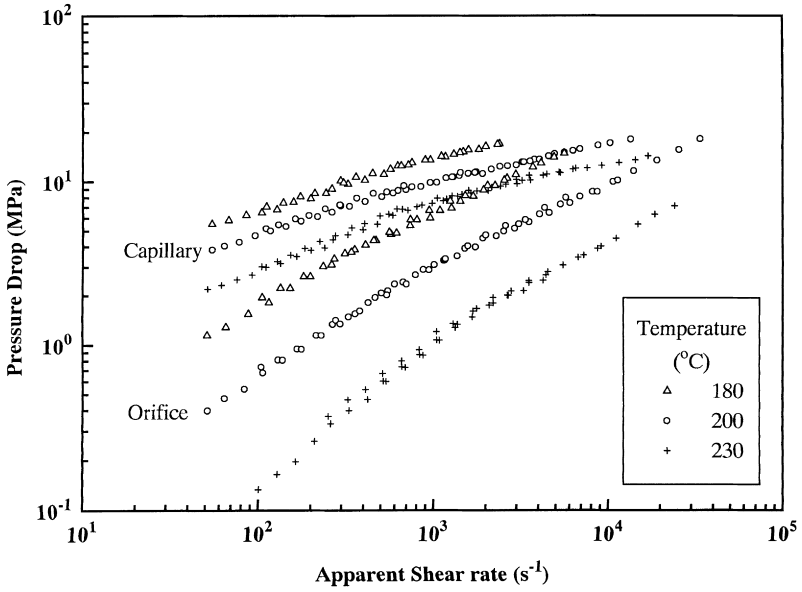

Fig. 8. Pressure reduced orifice and capillary data for PS at 170, 200 and 230°C.

6.3. High-density polyethylene

Tests on HDPE were conducted at the lower temperatures of 150, 170 and 200°C, because the orifice pressure drops become impossible to detect at higher temperatures. The resulting temperature and pressure coefficients, featured in Tables 1 and 2, are relatively low. Indeed, it is not surprising that the pressure dependence of HDPE is lower than that of LDPE, since the former polymer does not exhibit the branched structure of the latter. Only a small difference is apparent between the orifice and capillary pressure coefficients. The time–temperature–pressure superimposed data for HDPE are shown in Fig. 10. The extent of the pressure drop data is more limited here, than for the other polymers, particularly in the case of the orifice because the orifice pressure drops were too low to measure at the lowest flow rates. However, over the two decades of shear rates where the data is available the superposition is good.

6.4. Polypropylene

PP was tested at 190, 200 and 230°C as lower temperatures were not possible due to problems with crystallisation for this grade of PP at 180°C and below. Temperature and pressure coefficients for PP fall between those of LDPE and PS and here again there is no substantial difference between

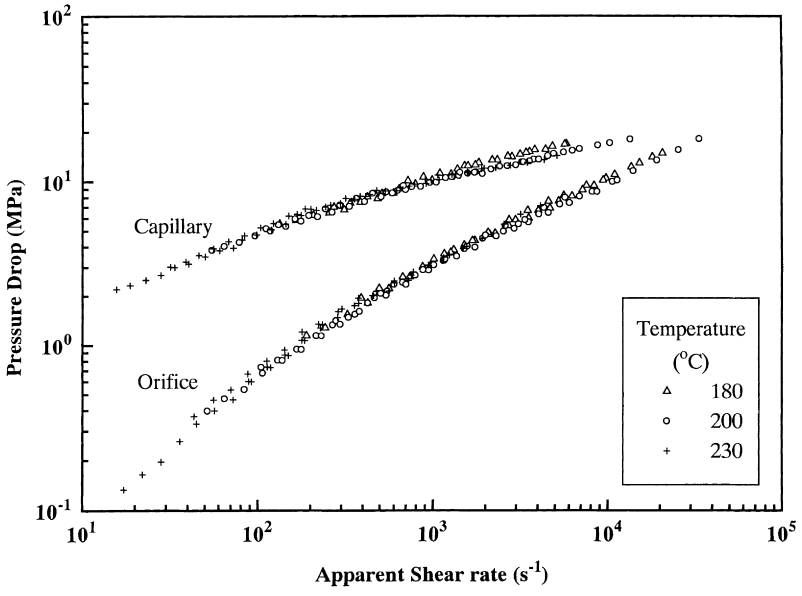

Fig. 9. Temperature and pressure reduced orifice and capillary data for PS.

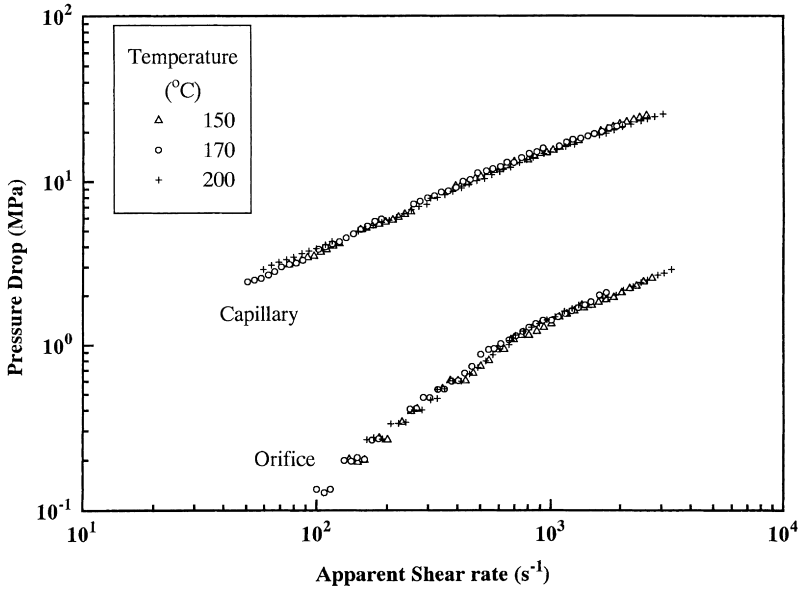

Fig. 10. Temperature and pressure reduced orifice and capillary data for HDPE.

the orifice and capillary values. The value of the shear pressure coefficient at 24.9 GPa^{-1} is in good agreement with the measurements of Kadjik and Van den Brule [14] who obtained a value of 23.5 GPa^{-1} for PP. Full superposition for PP is shown in Fig. 11.

6.5. Polymethyl methacrylate

PMMA is known to be very temperature sensitive and for this reason the PMMA samples were tested over a narrower band of temperatures between 220 and 240°C. The pressure coefficients for PMMA are second only, in magnitude, to those of PS (and lie between PP and PS). However, the temperature coefficients are even greater than those of the PS. This is interesting, since it is normally expected that materials with greater temperature dependence would also exhibit greater pressure dependence. For example, Cogswell [15] has stated "an increase in the pressure of a polymer melt was equivalent to a decrease in temperature and that if the viscosity (shear) was very sensitive to changes in temperature then a similar sensitivity to pressure could be anticipated". Though this is generally true of the other polymers investigated, PMMA appears to be an exception. The increase of the pressure coefficient in elongation over that in shear for the PMMA is small compared with the PS but does seem to be a little larger than for the polyolefines. However, it still falls within the scope of experimental uncertainty.

Fig. 12 shows the superimposed pressure drop data for

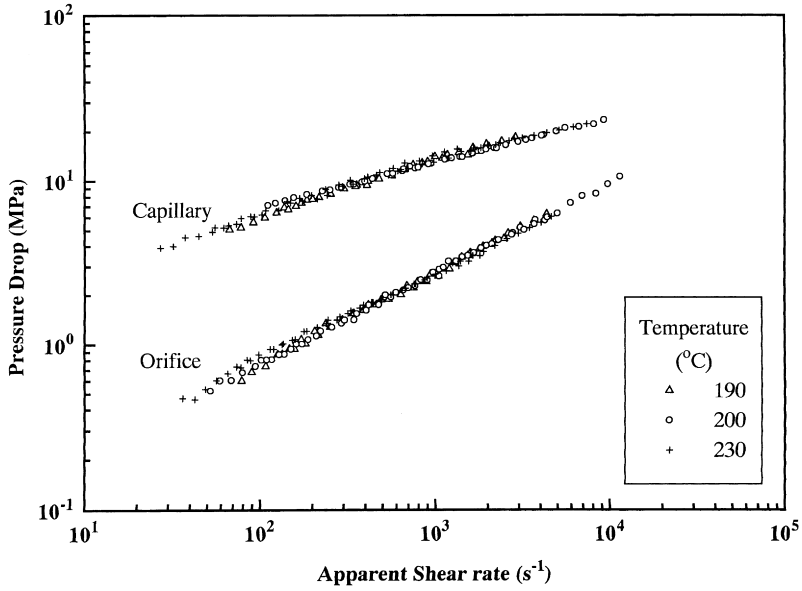

Fig. 11. Temperature and pressure reduced orifice and capillary data for PP.

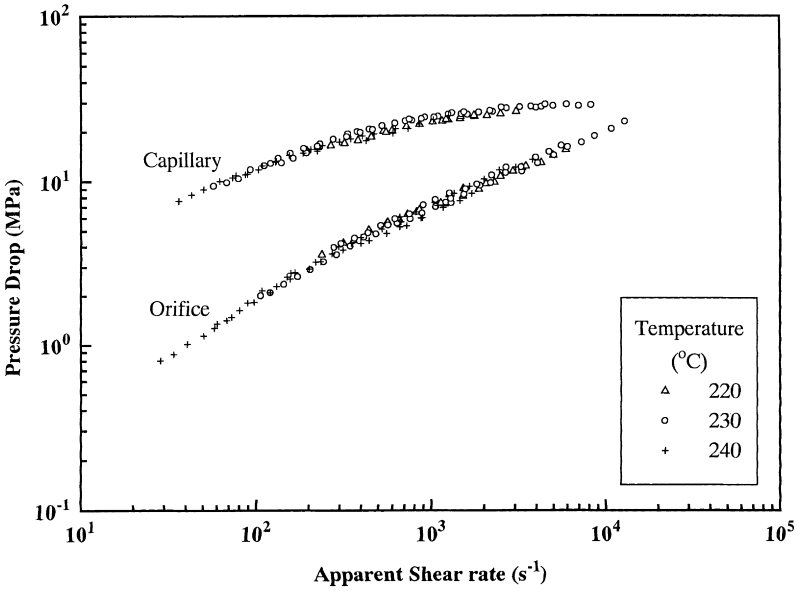

Fig. 12. Temperature and pressure reduced orifice and capillary data for PMMA.

PMMA, which are similar to those of the PS. Here again the level of fit is not quite as good as for the LDPE particularly for the orifice, but in this case it can be directly attributed to the sensitivity of the melt viscosity to small changes in temperature.

6.6. Discussion

In summary, examination of the temperature and pressure superimposed data reveals that good superposition is achieved for the LDPE and HDPE for both the orifice and capillary pressure drops and reasonable levels of superposition are obtained for the PS, PP and PMMA. In all cases, better superposition is observed with the capillary, mainly because the associated pressure drops are significantly larger and more accurately measurable than those for the orifice die. Therefore, allowing for experimental uncertainty, it can be concluded that, the time–temperature–pressure superposition holds in both shear and elongation for all of the polymer melts.

The pressure dependence of the melts as characterised by these shear and extensional pressure coefficients is ordered: PS > PMMA > PP > LDPE > HDPE. However, in terms of temperature dependence the ordering is: PMMA > PS > PP > LDPE > HDPE.

The ordering must be a direct consequence of the differences in the chemical structure of the individual polymers, since this is known to be responsible for the temperature/pressure dependence of polymer melts. HDPE, which has the lowest temperature and pressure dependence, has the simplest (linear) structure of the polymers. LDPE has the same chemical structure, but also has some degree of chain branching, that causes it to show greater dependence than HDPE. The remaining polymers PP, PMMA and PS have progressively larger pendant groups attached to their carbon chains and there is a direct correlation with this and their levels of pressure dependence. However, PMMA has the highest temperature dependence and we can only speculate that this may result from it having two pendant groups on each of its monomer units (see Fig. 1).

The error associated with the temperature and pressure coefficients of the polymers is typically within ±5% for shear and ±10% for elongation, based on the levels of fitting achieved with the superposition. As mentioned previously, in the case of the orifice, the levels of experimental scatter are high, because the measured pressure drops are very small compared with the pressure ratings of the transducers. Given these levels of experimental uncertainty, probably the most interesting result to arise from the tables is that, with the exception of PS that has significantly higher coefficients in elongation, the shear coefficients are at similar levels as those of elongation. Therefore, it can be concluded that for most polymers the temperature and pressure dependencies are essentially the same in both shear and elongation.

It is important to realise that although the pressure levels in the capillary and entry flow regions are high, the actual pressure drops associated with the capillary and orifice are relatively modest (usually (30 MPa) when compared with those encountered in, for example, injection moulding processes. Most of the major assumptions regarding the capillary flow analysis, such as incompressibility, negligible viscous heating and a linear pressure gradient, can be justified in terms of this fact, i.e. the pressure drops are no greater than those encountered in conventional capillary rheometry.

7. Conclusions

This paper is the second of a series that address the

Table 3
Shear and extensional pressure coefficients for the five oil samples

Oil	β_S (GPa^{-1})	β_E (GPa^{-1})
Oil A lub	23	22.5
Oil A (degraded)	22.5	23
Oil B lub	23	22.5
Oil B (degraded)	23.5	23.5
Single grade oil 2	24	24.5

important issue of the pressure dependence of rheological parameters in the case of commercially important non-Newtonian fluids. It deals mainly with the relationships between the temperature and pressure dependencies of shear and elongational flows and the use of superposition theory to estimate the relevant parameters.

Within the error limits of the experiments time–temperature–pressure superposition is found to hold for all the samples considered in both shear and elongation, although the degree of fit is best for HDPE and LDPE.

The temperature coefficients exhibit trends similar to those for pressure, however, the ordering of the temperature dependence differs in that, the PMMA has higher temperature coefficients (see Table 2) than the PS.

The most significant result is that for each polymer the shear temperature and pressure coefficients are of similar value (allowing for experimental uncertainty) to those of elongation, with the exception of PS that has considerably greater coefficients in elongation particularly for temperature. Therefore, this enables us to conclude that most polymers will have essentially the same temperature and pressure dependence in both shear and elongation flows.

Acknowledgements

The authors would like to thank the following people for their support in completing this paper: Professor K. Walters for his advice and support during the course of the project; Mr A.J. Palmer and Mrs C.M. Millichamp for their technical support and J. Christienson (of the Technical University of Denmark, Lyngby) for his help in establishing the experimental technique. Acknowledgement is also due to the DTI for its earlier support, through a LINK project, which led to the development of the prototype capillary rheometer, to ICI (Wilton, UK) for their co-operation in supplying some of the polymers and, last but not least, the EPSRC for providing the funding for the enhanced pressure research.

Appendix. Single and multigrade oils

In a follow up paper by the authors [16] the shear and elongational properties of a series of motor oils were investigated using the modified capillary rheometer. The study was restricted to regard the influence of pressure alone and so the temperature was maintained at an ambient one (20°C). Two multigrade oils 15W/40 were considered along with a single grade oil (having no polymer additive) for control purposes, degraded samples of the same multigrade oils were also tested. The degradation was achieved by repeatedly passing the oils through a fine diesel injector. Both oils designated as Oil A and Oil B were produced from the same base oil and differed only by the polymer additives used in their formulation.

The focus of the former paper was the effect of pressure on the Trouton ratios of the oils. However, by applying the time–pressure superposition to the raw capillary and orifice data it is possible to derive pressure coefficients from the resulting shift factors, as was done with the polymer melts above. These results were not reported in the 'oils paper', but are included in Table 3 because of their relevance to the current study. A truly fascinating finding, which is evident from the table, is that within experimental uncertainty the pressure coefficients for the single and multigrade oils (including the degraded samples) are always the same at 23.5 ± 1 GPa^{-1} in shear and 23.5 ± 2 GPa^{-1} in elongation. The error margins are marginally better than those of the melts simply because the temperature control of the instrument is tighter at 20°C than at, for example, 200°C. These values are very close to those of PP, which is in the middle of the range of the polymers considered. It is thought that the pressure coefficients of the oils are solely dependent on the base oil and, unlike those of the melts, do not vary when the polymer additive is changed, because of the relatively low concentrations of polymer involved. This is despite the fact that the polymer additives will have a marked effect on the rheology of the oils themselves, i.e. single grade oils are essentially Newtonian, while multigrade oils are highly viscoelastic and the degraded samples will also be viscoelastic but to a lesser extent (these findings are demonstrated in another paper [16]).

References

[1] Binding DM, Couch MA, Walters K. J Non-Newtonian Fluid Mech 1998;79:137.
[2] Barus C. Proc Am Acad 1891–1892;27:13.
[3] Vogel H. Physik Z 1921;22:645.
[4] Ferry JD. Viscoelastic properties of polymers. 3rd ed. New York: Wiley, 1980.
[5] Doolittle AK, Doolittle DB. J Appl Phys 1957;28:901.
[6] Carreau PJ, Choplin L, Clearmont JR. Polym Eng Sci 1985;25:669.
[7] Moldenaers P, Vermant J, Mewis J. J Rheol 1996;40:203.
[8] Bagley EB. J Appl Phys 1957;28:624.
[9] Bagley EB. Trans Soc Rheol 1961;5:355.
[10] Maia J, Binding DM. Rheol Acta 1999;38:160.
[11] Rabinowitsch B. Z Physik Chem (Leipzig) 1929;1:145.
[12] Penwell RC, Porter RS, Middleman S. J Polym Sci 1971;9:731.
[13] Laun HM. Rheol Acta 1983;22:171.
[14] Kadijk SE, van den Brule BHAA. Polym Eng Sci 1994;34:1535.
[15] Cogswell FN. Plast Polym 1973;41:39.
[16] Binding DM, Couch MA, Walters K. J Non-Newtonian Fluid Mech 1999;87:155.